Turbulence, Heat and Mass Transfer 8

CFD investigation of a Stirling engine flexi-fuel burner based on MILD combustion

A. Abou-Taouk[1,2], P. Wettrell[2] and L. E. Eriksson[3]

[1,3] *Chalmers University of Technology,*
Hörsalsvägen 7A, SE-41296 Gothenburg, Sweden, abdallah@chalmers.se, lee@chalmers.se

[2] *Cleanergy AB,*
Therese Svenssons gata 15, SE-41755, Gothenburg, Sweden, pontus.wettrell@cleanergy.com

Abstract — This paper presents comparisons of results from tests and 3D CFD combustion simulations based on both RANS and hybrid URANS/LES (SAS-SST model) turbulence models applied to an industrial Stirling engine combustion chamber at atmospheric pressure. The combustor uses both air preheating and exhaust gas recirculation. Both methane gas and landfill gas (24.2% CH_4, 21.6% CO_2, 2.0% O_2 and 52.2% N_2 by volume) were simulated. The combustor is designed to operate in the MILD combustion mode which is characterized by low flame temperatures and low NO_X emissions. A 4-step reduced reaction mechanism, named AAT4NR, involving seven species was developed to represent the landfill gas. The optimization was performed at atmospheric pressure for a range of fresh gas temperatures [300 K - 1000 K] and equivalence ratios [0.15 - 1]. Comparisons with detailed chemistry solutions of a planar propagating flame front show that the laminar flame speed, the adiabatic flame temperature, the ignition delay time and the species concentration at equilibrium are adequately predicted. There is good agreement between the quantities predicted with URANS/LES and experimental data, in terms of flow and flame dynamics, averaged temperatures, NO_X-levels and the concentrations of some major species.

1. Introduction

Combustion of fossil fuels has provided the major part of our energy needs in the past and will remain the dominating energy conversion process in the near future [1]. The reduction of pollutant emissions from practical combustion systems therefore is a major issue both in industry and in combustion research. Regulatory requirements for limiting emissions, such as nitrogen oxides (NO_X), carbon monoxide (CO) and unburned hydrocarbons (UHC), and the demand for higher efficiency combustion systems lead to new technologies of energy systems and combustors. These include, for example, premixed burners, air staging and exhaust gas recirculation (EGR). The growing trend today is that combustors should be fuel flexible. These different fuels are typically of Low Caloric Value (LCV), such as biofuels, syngas [2, 3] and landfill mixtures. The industrial company Cleanergy is the worlds's leading supplier of sustainable energy solutions based on the Stirling engine. The Stirling engine, described by [4], is a prime mover with energy input in the form of externally supplied heat. This can be done via e.g. a combustion chamber or a solar concentrator. Cleanergy has found a market niche towards LCV type of fuels and currently focuses on renewable, gaseous mixtures that are relatively difficult to burn since the energy content is small compared to natural gas. One such gas is Landfill gas. In a landfill gas extraction the methane content is decaying with time. The low methane content is often a limitation for conventional techniques, typically gas turbines and IC engines. Cleanergys newly developed and manufactured burner has shown capabilities to burn landfill gas and other types of LCV mixtures with very low energy content. The new burner (named GasBox, see Figure 1) is driving an alfa type Stirling engine where the burner is designed and manufactured at Cleanergy AB, Sweden. The engine power output is 7.2 kW electric power and 16 kW

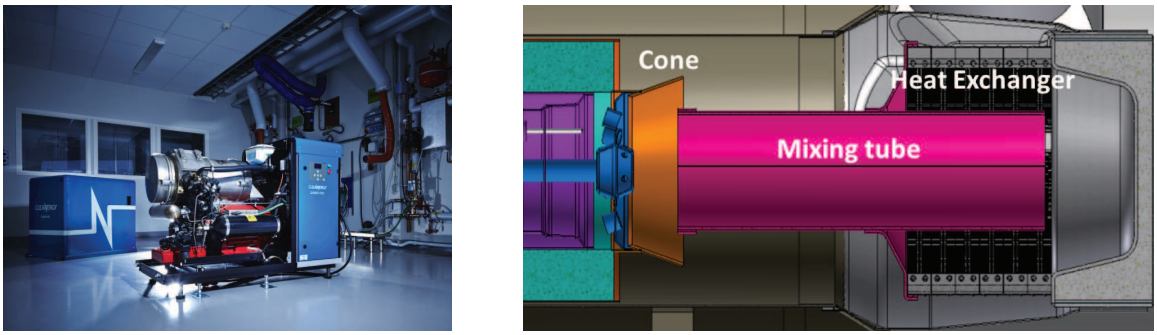

(a) GasBox inside view. (b) Centerline plane of the combustor.

Figure 1: Cleanergy GasBox and combustor.

heat power. The GasBox combustor provides extremely low NO_X levels with multi-fuel capability. The burner is based on a recently developed combustion technology, so-called Moderate or Intense Low Oxygen Dilution (MILD) combustion [5–7], also known as flameless oxidation or high temperature air combustion [8]. The MILD combustion regime is based on strong gas recirculation combined with air preheating which generates high combustion efficiency and relatively low flame temperatures. The air is diluted with a large amount of gas recirculation which implies that the mass fraction of oxygen in the reaction zone is much lower than in the case of undiluted air and therefore the reaction zone becomes distributed and no visible flame is obtained. The MILD combustion regime features a relatively low NO_X and CO emissions values [9, 10].

The GasBox burner, as shown in Figure 1, consists of a main burner and a heat exchanger. The gas is injected from one location and there are 6 main injection holes at the entrance of the burner. The main air is preheated above the auto-ignition temperature of the fuel. The air and the fuel are also diluted by exhaust gas recirculation. Turbulent combustion modeling is often based on flamelet or non-flamelet approaches [11]. Since the MILD combustion regime is relatively new the knowledge of the MILD reaction zone is still not fully understood. Different turbulent combustion models for MILD combustion have been used together with Reynolds Averaged Navier-Stokes (RANS) simulations [12–15] and Large Eddy Simulations (LES) [16, 17]. Finite rate chemistry models may become very important in MILD combustion regime since the moderate temperatures and the low oxygen content makes the reaction rates slower. Using detailed chemical kinetics in numerical 3D CFD simulations of this type of combustion system include many challenges and modelling issues both regarding computational strategy and resources. Current mechanisms in combination with detailed models provide good predictions of laminar flame speeds formed by light hydrocarbons such as methane. However, complexity and number of reactions increases significantly with heavier hydrocarbons and different kind of biofuels. Hence, this study focuses on the development of reduced chemistry for landfill gas that can be used with CFD in a more cost effective manner.

In the present work a set of reference laminar and one-dimensional premixed flames at various equivalence ratios are first simulated using detailed chemistry. Then, an optimization loop is set up to determine the best Arrhenius rates of the AAT4NR global reaction mechanism (consisting of 4 global reactions and 7 species), so that the reference flames are readily reproduced when the flames are computed with the AAT4NR global mechanism. The optimized AAT4NR mechanism is then implemented in the CFD software Ansys CFX, and computational results are obtained for the GasBox burner provided by Cleanergy AB. In the present CFD work the turbulence models k-ω - Shear Stress Transport (SST) and Scale Adaptive Simulation (SAS)-

SST have been used combined with the optimized AAT4NR global mechanism (see Table 1) for landfill gas and the M4 mechanism [18] for methane/air mixtures. All of the CFD simulations were carried out using the combined turbulence-chemistry interaction model named ″Eddy Dissipation Model (EDM)/Finite Rate Chemistry (FRC)″ in Ansys CFX, a short explanation of this model is given in section 3.

2. Kinetic optimization

Reduced chemistry is usually required in 3D turbulent reactive flow simulation since it is often limited by the run-time and convergence requirements. Global mechanisms are well suited for CFD simulations since they are based on Arrhenius rates and can be implemented easily into CFD codes. Several different reduced reaction mechanisms of methane-air mixture and propane can be found in the literature, see [18–20]. However, the number of reduced reaction mechanisms for LCV mixtures are very limited.

2.1. Optimization method

The optimization is performed first by choosing a set of N_{fl} one-dimensional and unstrained premixed flames that are computed with the detailed GRI-Mech 3.0 mechanism [21]. This is done for an ensemble of operating conditions, characterized for instance by the equivalence ratio and the fresh gases temperature. The data are saved to provide reference solutions. Second, the same set of flames is simulated by the 4-step AAT4NR mechanism shown in Table 1. The mechanism is valid for operating pressure condition of 1 bar, inlet temperatures from 295 - 1000 K and equivalence ratios from 0.15 to 1. Third, a fitness function is defined to measure and minimize the departure between the two set of solutions. The CHEMKIN software [22] has been used to solve the freely propagating premixed flame equations, and it was coupled with the optimization toolbox ModeFrontier [23]. The chosen flames are solved interactively with the optimization tool, until the fitness function reaches its minimum and the best set of parameters is determined, shown in Table 1. After defining ranges of search for all the parameters, the genetic algorithm [24] was applied to find the best set of parameters for the considered conditions. The chosen optimization method follows the same strategy as previously used by Abou-Taouk et al. [18] and Farcy et al. [25].

2.2. Results - AAT4NR mechanism

The AAT4NR mechanism has been optimized for the landfill mixture (24.2% CH_4, 21.6% CO_2, 2.0% O_2 and 52.2% N_2 by volume). The optimized mechanism consists of four global reactions visible in Table 1, including corresponding kinetic rate data.

Table 1: Kinetic rate data (units in cm, s, kcal and mole) for the AAT4NR global reaction mechanism using an operating pressure of 1 bar.

Reaction	A_i	B_i	E_{a_i}	Reaction order
$CH_4 + \frac{1}{2} O_2 \rightarrow CO + 2H_2$	2.2E+15	-0.1	40.5	$[CH_4]^1$, $[O_2]^1$
$H_2 + \frac{1}{2} O_2 \rightarrow H_2O$	2.08E+18	0.5	42.0	$[H_2]^{1.2}$, $[O_2]^{0.9}$
$CO_2 \rightarrow \frac{1}{2} O_2 + CO$	1.0E+11	-0.5	42.75	$[CO_2]^1$
$CO + H_2O \rightarrow CO_2 + H_2$	6.0E+14	-0.4	40.0	$[CO]^{0.6}$, $[H_2O]^{0.7}$

Figure 2 shows the laminar flame speed and the ignition delay time at atmospheric pressure. It is confirmed that the optimization loop has provided a system of equations which propagate the flame front close to the flame speed obtained with the detailed chemical mechanism. Figure 2 shows also the ignition delay time predicted by different global reaction mechanisms: the 2-step mechanism (WD2) by Westbrook and Dryer [19], the 4-step mechanism (JL4) by Jones and Lindstedt [26] and the 3-step mechanism (M3) by Meredith et al. [20]. It is clear that the new optimized 4-step AAT4NR mechanism predicts the ignition delay time reasonably well compared to the detailed mechanism and considerably better than the other global reaction mechanisms. Figure 3 shows the detailed GRI-Mech 3.0 equilibrium species concentrations and the adiabatic temperature at different equivalence ratios, together with the reduced AAT4NR mechanism counterpart. It is seen that the AAT4NR mechanism captures the equilibrium conditions and the adiabatic temperature very well for the considered range.

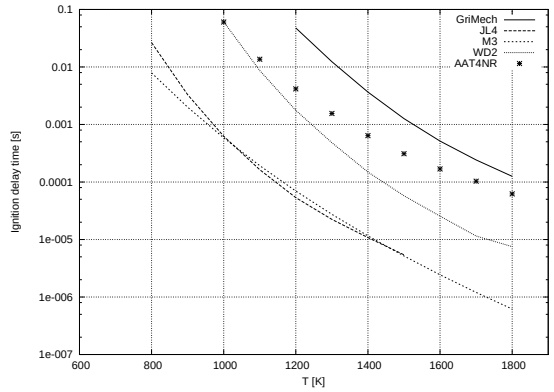

(a) Ignition delay time vs. T for different global mechanisms.

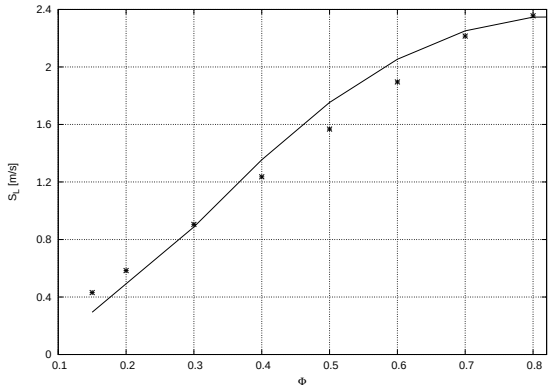

(b) Laminar flame speed vs. ϕ. Symbols: AAT4NR mechanism, solid-line: detailed mechanism.

Figure 2: Ignition delay time and laminar flame speed using different global mechanisms compared to the detailed mechanism; landfill mixture.

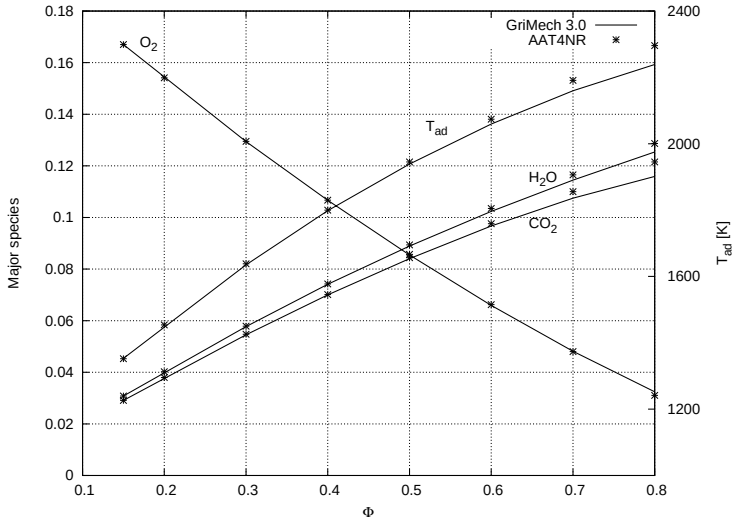

Figure 3: Equilibrium concentrations (mole fractions) of the species and the adiabatic flame temperatures vs. ϕ using the present AAT4NR mechanism compared to the detailed GRI-Mech 3.0 mechanism; landfill mixture.

3. Reaction rate calculation

MILD combustion is based on relatively low temperatures and a high amount of dilution. These together make reaction rates slower than conventional flames and consequently lower Damköhler number. Hence, both the mixing and the finite rate chemistry models may become important in the MILD combustion regime. There exist different combustion models that take this effect into account, namely the Eddy Dissipation Concept (EDC) and the combined EDM/FRC model. Reasonable good agreement was shown by Christo & Dally [13] and Sarras et al. [15] using the EDC model. In this work, the combined turbulence-chemistry interaction model, that is the EDM/FRC, in Ansys CFX, is chosen for the CFD simulations. The advantage of this model is that the reaction rates can be limited by turbulent mixing in some regions of the domain and limited by kinetics in other areas in the domain.

The FRC model computes the reaction rate based on the following expression:

$$\dot{\omega}_i = A_i \prod_{j \in \mathcal{A}_i} \left(\frac{\rho Y_j}{W_j} \right)^{\mu_{j,i}} T^{B_i} \exp\left(-E_{a_i}/(\mathcal{R}T)\right) \ , \tag{1}$$

where $\mathcal{A}_i$ is the ensemble of species involved in reaction i, ρ denotes the density, $\mathcal{R}$ denotes the universal gas constant, W_j is the molecular weight of species j, B_i is the temperature exponent, E_{ai} is the activation energy, A_i is the pre-exponential factor and $\mu_{j,i}$ is the reaction orders of species j in reaction i. The FRC model computes one reaction rate for each individual reaction used in the global reaction mechanism. In the EDM model the reaction rate of reaction i is computed as:

$$\dot{\omega}_i = A_i \frac{\epsilon}{k} \prod_{j \in \mathcal{A}_i} min\left(\frac{[I]}{\mu'_{j,i}} \right) \ , \tag{2}$$

where $\frac{\epsilon}{k}$ is the turbulent mixing rate and $[I]$ is the molar concentration of component i. The EDM model computes one reaction rate respectively for each reaction in the global reaction mechanism. The EDM-FRC model thus selects the minimum rate from the two models. The reaction rates in the present 4-step mechanism are expressed following equation 1.

4. Computational details and burner case

4.1. Flow path

Figure 4 shows a schematic picture of the GasBox burner and the CFD-domain used in the simulations. The fuel and the air are mixed together with the EGR mixture in the prechamber upstream of the mixing tube. This mixture is spontaneously ignited. The mixing is achieved by aligning the fuel jet towards the air jet. MILD combustion is obtained in the mixing tube where a small temperature variations are achieved, see Figure 5. The mixture then makes a 180 degree turn downstream the mixing tube and then pass the heat exchanger. Finally, the mixture continuous backwards towards the outlet where a portion is directed by the cone back to the prechamber and a portion is leaving the domain through the outlet.

4.2. Numerical implementation

The CFD software Ansys CFX was used for all simulations. ANSYS CFX software uses a coupled solver and the solution approach uses a fully implicit discretization of the equations at any given time step. The high resolution scheme (which is a bounded second-order upwind biased discretization) was applied for discretization in space and time. The mesh is composed of 1.5

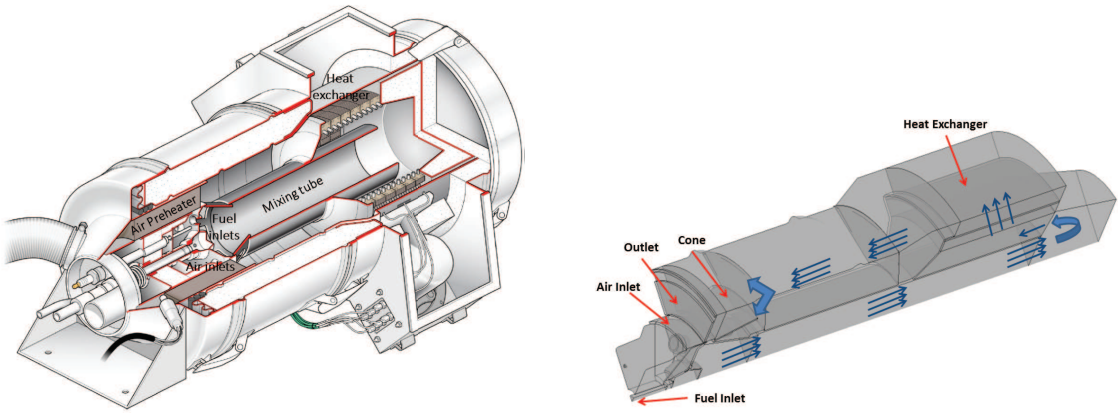

(a) (b)

Figure 4: Left: GasBox cut showing the burner. Right: CFD-domain of the combustor.

million hexahedral cells. The turbulence models k-ω-SST has been used for all RANS simulations and the SAS-SST used for the transient simulation. The chemistry was represented by the new AAT4NR global mechanism for landfill gas and the M4 mechanism [18] for methane/air mixture. Results are presented with the inclusion of radiative heat transfer.

4.3. Simulation parameters

The CFD-domain is shown in Figure 4b. Specified mass flow rates are imposed at the inlet boundaries for the air inlet and the fuel inlet. The preheated air temperature is set to 1000 K at the air inlet and 320 K for the fuel inlet. The outlet boundary condition is set to 1 bar and a no-slip adiabatic boundary condition is imposed on all walls. The P1 model for radiation was included in the CFD simulations leading to an additional transport equation to be solved. The global ϕ in the burner is approximately 0.2 including the EGR mixture. The heat exchanger is included in the CFD simulations were a heat sink is introduced in order to represent the amount of the heat that is extracted by the heat exchanger in the Stirling engine.

For the transient simulations, the statistics are first converged for a non-reactive case, and the flow is then advanced in time with combustion for about 0.5 s (ten flow-through times) until the flame is well established and statistics are accumulated for another 0.5 s. The time step for the simulation was set to 1.0e-4 s which implies a mean CFL number of 1. Conservation checks were made for mass, momentum, energy and major species. For the steady-state simulations, the mass was within $\pm 0.5\%$, energy within $\pm 0.1\%$, momentum within $\pm 0.001\%$ and major species within $\pm 0.5\%$. Different monitor points were also positioned at different locations in the burner to check that convergence had been obtained in the burner.

5. CFD results and discussions

5.1. RANS

Figure 5 shows a contour plot of the normalized temperature of natural gas and the considered landfill mixture. The temperature is normalized by the maximum temperature of each considered mixture. The peak temperature difference in the plots is about 1000 K. It is clear that the natural gas case is burning with a flame with high peak temperatures and consequently high NO_X levels, 180ppm. Using the inlet temperature $T_{in} = 1000$ K, Oberlack et al. [27] wrote that the temperature increase due to heat release should not exceed 25% of the inlet temperature if MILD combustion regime is to be obtained (this is based on one reaction with activation energy

of 40kcal/mole). The $\Delta T/T_{in}$ for natural gas is much higher than this value, approximately 140 $\%$. For the present landfill gas mixture the ratio $\Delta T/T_{in}$ is around 30$\%$ and closer to the value needed to maintain MILD combustion mode. The RANS simulation for landfill mixture

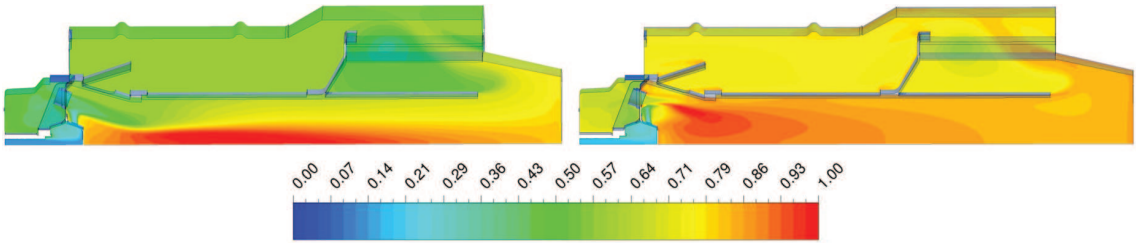

Figure 5: Normalized temperature: left-natural gas, right-landfill mixture. The difference in peak temperature between the two plots is about 1000 K.

shows a more uniform temperature distribution and a distinct reaction zone is visible which is expected considering the MILD combustion mode. The uniform temperature leads to the reduction of peak temperature which implies that the formation of NO_X is largely suppressed, visible in Figure 6. Comparing the NO_X concentration distributions of both of the simulated cases it is obvious that in the landfill case a small amount of NO_X is created in a large volume of the mixing tube, opposed to the natural gas case were the most of the produced NO_X is originating from the hot flame zone close to centerline downstream the mixing tube (the red color region in the left plot of Figure 6).

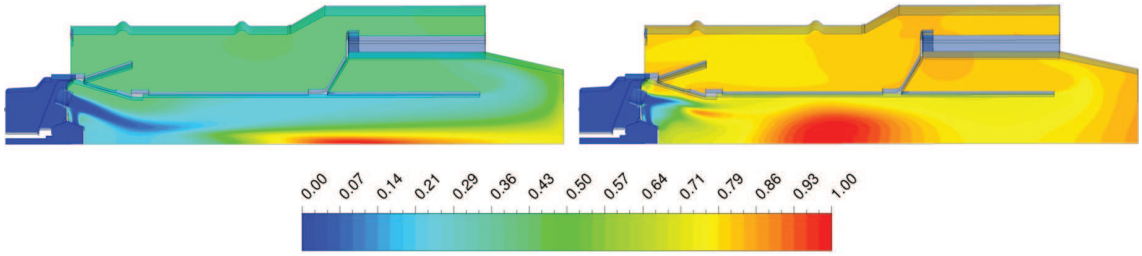

Figure 6: Normalized NO_X: left-natural gas, right-landfill mixture. The NO_X concentration is normalized by the peak NO_X concentration of each considered mixture. The difference in peak values between the two plots is about 400 ppm.

5.2. URANS/LES

The advances in computing power and numerical schemes allow hybrid URANS/LES and LES to be used more. This makes it possible to use more detailed turbulent combustion models applied to real industrial combustor cases. The SAS-SST model [28] is a hybrid URANS/LES model and is used for the transient simulation in Ansys CFX. This model switches to LES mode in unsteady flow if the resolution of the grid is sufficient and to an unsteady RANS mode close to the walls. The von Karman length scale explicitly enters the transport equations to the SAS model. The model gives suitable RANS solutions for stable flows. For flows with transient behavior, the model reduces its eddy viscosity according to the locally resolved vortex size represented by the von Karman length scale. The SAS model can under those conditions allow the break-up of large unsteady structures into a turbulent spectrum and avoid RANS-typical single-mode vortex structures. Figure 7 shows an instantaneous snapshot of the normalized temperature (left) and a mean normalized temperature plot (right) using the present AAT4NR mechanism for the landfill mixture. The temperature contours show that the main combustion

zone is located inside the combustion chamber without wall attachment. It can be seen that while some reaction takes place inside the prechamber the majority of the heat is released inside the combustion chamber distributed relatively equally.

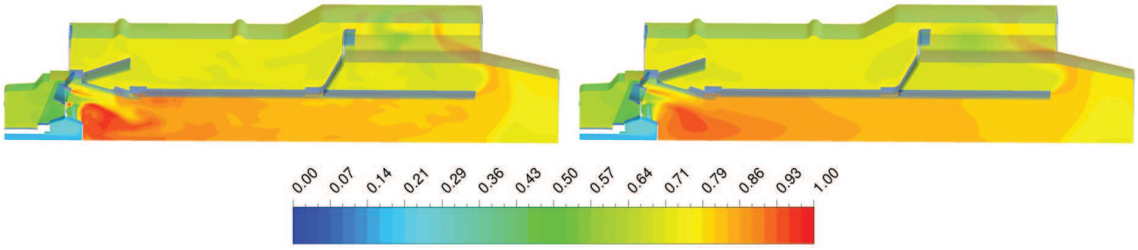

Figure 7: Snapshot of the instantaneous normalized temperature (left) and time-averaged normalized temperature (right) using the AAT4NR mechanism and the SAS-SST turbulence model for the landfill mixture.

Snapshots of the instantaneous velocity magnitude (left) and the mean velocity contours (right) in the combustor mid-plane are presented in Figure 8 for the landfill mixture. High levels of turbulence and mixing are found in the prechamber due to the complex flow arrangement in this region. The contour plots of the velocities identifies toroidal recirculation zone in the corner of the prechamber combustion region. The velocity field shows a high velocity jet region that starts from the air inlet and continues into the mixing tube.

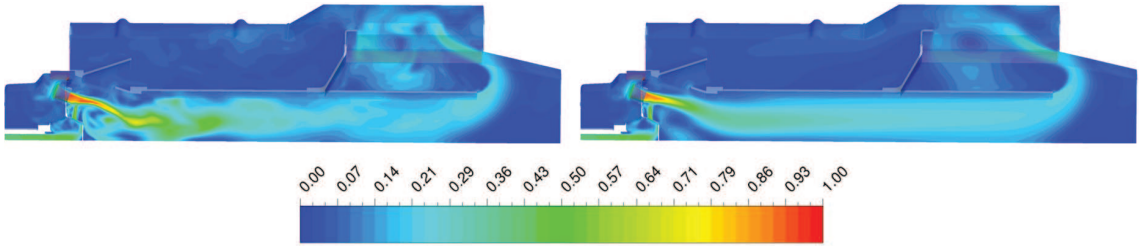

Figure 8: Snapshot of the instantaneous normalized velocity (left) and time-averaged normalized velocity (right) using the AAT4NR mechanism and the SAS-SST turbulence model for the landfill mixture.

Table 2 shows a comparison between predicted CFD data (both RANS and URANS/LES) and measurements. The first thing to note is that the SAS model predicts emissions and NO_X better compared to RANS. This is consistent with previous studies by Lörstad et al. [29] and Abou-Taouk et al. [18]. The reason for this is due to that the RANS underpredicts the temperature in comparison with the more transient calculations. A lower temperature gives a lower NO_X prediction since the NO_X concentration is strongly linked to the temperature. The prediction of the transient CFD simulation shows a good agreement with measured data.

Table 2: Major emissions and mean NO_X concentrations: experimental data compared to CFD.

Emissions	Experiment	CFD k-ω-SST	CFD SAS-SST
Landfill: CO_2	17.4%	15.3%	16.1%
Landfill: O_2	7.3%	7.4%	7.0%
Landfill: NO_X	$<$ 10ppm	$<$ 1ppm	$<$ 10ppm
Natural gas: NO_X	150ppm	—	180ppm

6. Summary

A new optimized global reaction mechanism, AAT4NR, was developed for the present landfill mixture (24.2% CH_4, 21.6% CO_2, 2.0% O_2 and 52.2% N_2 by volume). The parameters of the 4-step AAT4NR global mechanism have been automatically obtained from the optimization loop for a range of equivalence ratios and inlet temperatures. The optimized Arrhenius rates allows for capturing the major species, the laminar flame speed, the adiabatic flame temperature and the ignition delay time for different equivalence ratio compared to a detailed reaction mechanism. Then, this new optimized global mechanism is used in RANS and URANS/LES modeling applied to an industrial Stirling engine combustion chamber at atmospheric pressure. The flow and flame properties are compared to measurements and reasonable agreement is seen in terms of major emissions, NO_X and temperatures.

Acknowledgements

The work by Chalmers University is funded by the Swedish Governmental Agency for innovation systems VINNOVA under Grant No. 2014-02282. The work performed by Cleanergy AB is partly funded by the Swedish Energy Agency through Energiforsk (former Swedish Gas Technology Center, SGC) under Grant No. 2014-000304, Project 38709-1. The authors also would like to acknowledge Cleanergy AB, for their permission to publish this paper.

References

[1] P. Grundy. Shell energy scenarios to 2050 , 2008.

[2] A. Abou-Taouk, I. Sigfrid, R. Whiddon and L. E. Eriksson. A Four-Step Global Reaction Mechanism for CFD Simulations of Flexi-Fuel Burner for Gas Turbines. In 7^{th} *International Symposium on Turbulence, Heat and Mass Transfer*, pp. 785–788, 2012.

[3] I. Sigfrid, R. Whiddon, R. Collin and J. Klingmann. Influence of reactive species on the lean blowout limit of an industrial DLE gas turbine burner. *Combustion and Flame*, 161(5):1365–1373, 2014.

[4] A. Organ. The Regenerator and the Stirling Engine along a Vertical Heated Plate. *Mechanical Engineering Publications Ltd*, London, 1997.

[5] M. de Joannon, G. Langella, F. Beretta, A. Cavaliere and C. Noviello. In *Proc. of Mediterranean Combustion Symposium*, pp. 347360, 1999.

[6] A. Cavaliere and M. de Joannon. In *Prog. Energy Combust. Sci.*, 30:329–366, 2004.

[7] P. Li and J. Mi and B. Dally and F. Wang and L. Wang and Z. Liu and S. Chen and C. Zheng. In *Science China Technological Sci.*, 54(2):255–269, 2011.

[8] J. A. Wünning and J. G. Wünning. *Prog. Energy Combustion Science*, 23:81–94, 1997.

[9] M. de Joannon and G. Sorrentino and A. Cavaliere. *Comb. Flame*, 159(5):1832–1839, 2012.

[10] C. Duwig and B. Li and Z. Li and M. Aldén. *Comb. Flame*, 159(1):306–316, 2012.

[11] D. Veynante and L. Vervisch. *Turbulent combustion modeling*, VKI LS Course, 2011.

[12] P. J. Coelho and N. Peters. *Comb. Flame*, 124:503–518, 2001.

[13] F. C. Christo and B. B. Dally. *Comb. Flame*, 142:117–129, 2005.

[14] C. Galletti and A. Parente and L. Tognotti. *Comb. Flame*, 151(4):649–664, 2007.

[15] G. Sarras and Y. Mahmoudi and L. D. Arteaga Mendez and E.H. van Veen and M. J. Tummers and D. J. E. M. Roekaerts. Modeling of Turbulent Natural Gas and Biogas Flames of the Delft Jet-in-Hot-Coflow Burner: Effects of Coflow Temperature, Fuel Temperature and Fuel Composition on the Flame Lift-Off Height. *Flow Turbulence Comb.*, 2014.

[16] C. Duwig and D. Stankovic and L. Fuchs and G. Li and E. Gutmark. *Comb. Sci. Technol.*, 180:279–95, 2008.

[17] M. Ihme and Y. C. See. *Proc. Combust. Inst.*, 33:1309–1317, 2012.

[18] A. Abou-Taouk, S. Sadasivuni, D. Lörstad and L. E. Eriksson. Evaluation of global mechanisms for LES analysis of SGT-100 DLE combustion system. In *ASME Turbo Expo*, GT2013-95454, San Antonio, USA, 2013.

[19] C. K. Westbrook and F. L. Dryer. *Progress in Energy and Combustion Science*, 10(1):1–57, 1984.

[20] K. V. Meredith and D. L. Black *44-th AIAA-Paper.–Reno, Nevada*, pages 1–13, 2006.

[21] G. P. Smith, D. M. Golden, M. Frenklach, N. W. Moriarty, B. Eiteneer, M. Goldenberg, C. T. Bowman, R. K. Hanson, S. Song, W. C. Gardiner, V. V. Lissianski, and Z. Qin. Technical report, 1999. http://www.me.berkeley.edu/gri-mech/.

[22] CHEMKIN, 2015. http://www.reactiondesign.com.

[23] modeFRONTIER, 2015. http://www.modefrontier.com.

[24] N. M. Razali and J. Geraghty. Genetic algorithm performance with different selection straggles in solving TSP. In *Proceedings of the World Congress on Engineering*, volume II, London, 2011. WCE.

[25] B. Farcy, A. Abou-Taouk, L. Vervisch, P. Domingo, and N. Perret. Two approaches of chemistry downsizing for simulating selective non catalytic reduction DeNOx process. *Fuel*, 118:291–299, 2014.

[26] W. P. Jones and R. P. Lindstedt. *Combustion and Flame*, 73:233–249, 1988.

[27] M. Oberlack and R. Arlitt and N. Peters. *Combustion Theory Modell*, 4:495–509, 2000.

[28] Y. Egorov and F. R. Menter. Development and Application of SST-SAS Turbulence Model in the DESIDER Project. *Second Symposium on Hybrid RANS-LES Methods*, Corfu, Greece, 2007.

[29] D. Lörstad and A. Lindholm and D. Barhaghi and E. Fedina and C. Fureby and A. Lantz and M. Aldén and A. Bonaldo. Measurements and LES of a SGT-800 Burner in a Combustion Rig. In *ASME Turbo Expo*, GT2012-69936, 2012.